Murphy, K. P., Privalov, P. L., & Gill, S. J. (1990) *Science 247*, 559-561.
Rashin, A. A. (1984) *Biopolymers 23*, 1605-1620.
Richardson, J. S. (1981) *Adv. Protein Chem. 34*, 167-339.
Roder, H., Elove, G. A., & Englander, S. W. (1988) *Nature 335*, 700-704.
Shäfer, L., Klimkowski, V. J., Momany, F. A., & Chuman, H. (1984) *Biopolymers 23*, 2335-2347.
Shoemaker, K. R., Kim, P. S., Brems, D. N., Marqusee, S., York, E. J., Chaikin, I. M., & Baldwin, R. L. (1985) *Proc. Natl. Acad. Sci. U.S.A 82*, 2349-2353.
Shrake, A., & Rupley, J. A. (1973) *J. Mol. Biol. 79*, 351-371.
Skolnick, J., & Kolinski, A. (1989) *J. Mol. Biol. 212*, 787-817.
Stanfield, R. L., Fieser, T. M., Lerner, R. A., & Wilson, I. A. (1990) *Science 248*, 712-719.
Taketomi, H., Ueda, Y., & Gō, N. (1975) *Int. J. Pept. Protein Res. 7*, 445-459.
Udgonkar, J. B., & Baldwin, R. L. (1988) *Nature 335*, 694-699.
Unger, R., Harel, D., Wherland, S., & Sussman, J. L. (1989) *Proteins: Struct., Funct., Genet. 5*, 355-373.
Vâsquez, M., & Scheraga, H. A. (1985) *Biopolymers 24*, 1437-1447.
Volwerk, J. J., & de Haas, G. H. (1982) in *Lipid-Protein Interactions* (Jost, P. C., & Griffith, O. H., Eds.) Vol. 1, pp 69-149, Wiley, New York.
Wetlaufer, D. B. (1973) *Proc. Natl. Acad. Sci. U.S.A. 70*, 697-701.
Wright, P. E., Dyson, H. J., & Lerner, R. A. (1988) *Biochemistry 27*, 7167-7175.

Site-Specific Mutagenesis of Conserved Residues within Walker A and B Sequences of *Escherichia coli* UvrA Protein†

Gary M. Myles,‡,§ John E. Hearst,‖ and Aziz Sancar*,‡

Department of Biochemistry and Biophysics, University of North Carolina School of Medicine, Chapel Hill, North Carolina 27599-7260, and Department of Chemistry and Division of Chemical Biodynamics, Lawrence Berkeley Laboratory, University of California, Berkeley, Berkeley, California 94720

Received November 8, 1990; Revised Manuscript Received January 15, 1991

ABSTRACT: UvrA is the ATPase subunit of the DNA repair enzyme (A)BC excinuclease. The amino acid sequence of this protein has revealed, in addition to two zinc fingers, three pairs of nucleotide binding motifs each consisting of a Walker A and B sequence. We have conducted site-specific mutagenesis, ATPase kinetic analyses, and nucleotide binding equilibrium measurements to correlate these sequence motifs with activity. Replacement of the invariant Lys by Ala in the putative A sequences indicated that K37 and K646 but not K353 are involved in ATP hydrolysis. In contrast, substitution of the invariant Asp by Asn in the B sequences at positions D238, D513, or D857 had little effect on the in vivo activity of the protein. Nucleotide binding studies revealed a stoichiometry of 0.5 ADP/UvrA monomer while kinetic measurements on wild-type and mutant proteins showed that the active form of UvrA is a dimer with 2 catalytic sites which interact in a positive cooperative manner in the presence of ADP; mutagenesis of K37 but not of K646 attenuated this cooperativity. Loss of ATPase activity was about 75% in the K37A, 86% in the K646A mutant, and 95% in the K37A-K646A double mutant. These amino acid substitutions had only a marginal effect on the specific binding of UvrA to damaged DNA but drastically reduced its ability to deliver UvrB to the damage site. We find that the deficient UvrB loading activity of these mutant UvrA proteins results from their inability to associate with UvrB in the form of $(UvrA)_2(UvrB)_1$ complexes. We conclude that UvrA forms a dimer with two ATPase domains involving K37 and K646 and that the work performed by ATP hydrolysis is the delivery of UvrB to the damage site on DNA.

(A)BC excinuclease is the enzymatic activity resulting from the coordinated action of UvrA, UvrB, and UvrC proteins which excise a wide variety of modified nucleotides from DNA by hydrolyzing the eighth phosphodiester bond 5′ and the fifth phosphodiester bond 3′ to the damaged base (Sancar & Sancar, 1988; Grossman & Yeung, 1990; Van Houten, 1990). A current model for the reaction mechanism is as follows (Orren & Sancar, 1989, 1990). UvrA, which is an ATPase and a DNA binding protein with higher affinity for damaged DNA than for undamaged DNA (Seeberg & Steinum, 1982), interacts with UvrB to form a $(UvrA)_2(UvrB)_1$ complex. UvrA delivers UvrB (which has a cryptic ATPase activity and no affinity for DNA) to the damage site and dissociates from the UvrB-damaged DNA complex. UvrC binds to this complex and either directly or indirectly mediates the dual single-strand DNA incisions. ATP binding and hydrolysis by UvrA and UvrB (which becomes activated in the ternary UvrA-UvrB-DNA complex; Seeley & Grossman, 1989, 1990) are required during several stages of the overall reaction. This study is aimed at characterizing the ATPase activity of UvrA and its role in specific steps of the excision nuclease activity.

† This work was supported by Grants GM32833 from the National Institutes of Health and PCM351212 from the National Science Foundation and in part by a grant CTR1872 from the Council for Tobacco Research Inc. and by U.S. Department of Energy Grant DE-AC03-76SF-00098.

* Correspondence should be addressed to this author.
‡ University of North Carolina School of Medicine.
§ Present address: Fred Hutchinson Cancer Research Center, 1124 Columbia St., Seattle, WA 98104.
‖ University of California, Berkeley.

0006-2960/91/0430-3824$02.50/0

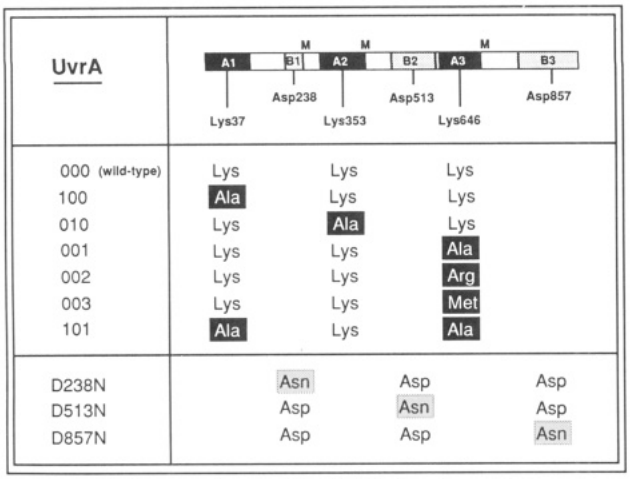

FIGURE 1: Point mutations in UvrA's Walker A and B homologous regions. (M denotes a metal binding Zn finger motif.)

Sequence analyses of the *uvrA* gene and protein revealed three nucleotide binding motifs (each comprised of a single Walker A and B sequence; Walker et al., 1982) interspersed with two intact and one partial zinc finger (Husain et al., 1986; Doolittle et al., 1986; Figure 1). This has led to the proposal that the *uvrA* gene evolved from the fusion of a primordial ATPase and a zinc finger gene followed by several gene duplication events. Furthermore, a comparison of UvrA's sequence with the sequences of several other ATPases revealed that the internal homology extends far beyond the Walker A (GXGXXGKS) and B ($\alpha\alpha\alpha\alpha$D, α = hydrophobic) sequences to include about 125 amino acids surrounding each of the Walker A and B sequences. Thus, it was proposed that the ATPase functional unit is comprised of two amino acid stretches, i.e., the A and B segments which contain the Walker A and B sequences, respectively. It was also suggested that these segments must fold independently and could, therefore, be referred to as domains (Doolittle et al., 1986; Higgins et al., 1986). While the sequence comparison provided compelling evidence for the presence of multiple ATPase sites in UvrA, direct experimental evidence has been lacking. In this study, we have conducted kinetic and equilibrium measurements to investigate the nucleotide binding sites in UvrA. We have mutagenized invariant residues in all six Walker A and B sequences in an effort to correlate the sequence of this protein with its structure and function. Our data suggest that UvrA has two ATP binding/hydrolysis functional domains which interact cooperatively in the presence of ADP and that each of these domains plays a critical role in loading UvrB onto damaged DNA by promoting the formation of $(UvrA)_2(UvrB)_1$ complexes.

Materials and Methods

Materials. UvrB and UvrC proteins were purified essentially as described by Thomas et al. (1985). Restriction enzymes, T4 kinase, and bacterial alkaline phosphatase were purchased from Bethesda Research Laboratories. T4 DNA polymerase and T4 ligase were from Bio-Rad, and Sequenase was from United States Biochemicals.

The radiolabeled nucleotides [2,8-^{3}H]ATP (30 Ci/mmol), [2,8-^{3}H]ADP (25.4 Ci/mmol), and [γ-^{32}P]ATP (7000 Ci/mmol) were from ICN Biomedicals, Inc. [α-^{32}P]dATP (800 Ci/mmol) was from New England Nuclear.

The chromatography resins were obtained from the following sources: AcA-22 and AcA-34 from IBF Biotechniques, BioGel P-10 and DEAE-BioGel from Bio-Rad, and single-strand DNA–cellulose and Blue Sepharose from Sigma. The thin-layer chromatography plates, Polygram cel300 poly(ethylenimine) (non-UV), were purchased from Brinkmann Instruments.

The plasmid and phage vectors pIBI24, pKK233-2, and M13K07 were obtained from IBI, Pharmacia, and Dr. C. Hutchison (University of North Carolina), respectively. The *Escherichia coli* K-12 derivatives used in this work were CJ236 (Kunkel et al., 1987), NM522 (Pharmacia), and UNC522 (Navaratnam et al., 1989).

Buffers. The following buffers were used: TEN 7.4, 10 mM Tris-HCl, pH 7.4, 1 mM EDTA, and 10 mM NaCl; lysis buffer, 50 mM Tris-HCl, pH 8.0, 100 mM NaCl, 1 mM EDTA, 10 mM 2-mercaptoethanol, and 10% sucrose; core buffer, 50 mM Tris-HCl, pH 7.5, 1 mM EDTA, and 20% glycerol, storage buffer, 50 mM Tris-HCl, pH 7.5, 100 mM KCl, 1 mM EDTA, 2 mM dithiothreitol, and 50% glycerol; ATPase buffer, 50 mM Tris, pH 7.5, 100 mM KCl, 10 mM $MgCl_2$, 5 mM dithiothreitol, and 100 μg/mL bovine serum albumin; (A)BC excinuclease buffer, 50 mM Tris-HCl, pH 7.5, 50 mM KCl, 10 mM $MgCl_2$, 5 mM dithiothreitol, and 50 μg/mL bovine serum albumin.

Construction of Point Mutants. Template for site-specific mutagenesis was prepared from CJ236/pUNC1940; this plasmid carries the *uvrA* gene on an *Nco*I–*Pst*I cassette inserted into the polylinker region of pIBI24N (a pIBI24 derivative with an *Nco*I site in the *Sma*I site of the polylinker). The site-specific mutations were introduced by the method of Zoller and Smith (1983) as modified by Kunkel et al. (1987). The mutants were identified by dideoxy sequencing (Sanger et al., 1977) using Sequenase (Tabor & Richardson, 1987) in place of Klenow fragment and were expressed by subcloning the mutant genes into the *Nco*I–*Pst*I site of pKK233-2.

In Vivo Complementation. The ability of mutant UvrA proteins to complement a *uvrA*$^-$ mutation was tested by introducing the plasmids carrying the mutant genes into UNC522 (*uvrA*::Tn10) and measuring the UV survival of the transformants after exposure to 15 J m^{-2} of 254-nm light from a germicidal lamp. Subtle differences in UV sensitivity between the wild type and mutants were detected by UV survival conducted over a dose range of 25–150 erg/mm^2.

Purification of UvrA Point Mutants. The wild-type protein, which we will refer to as UvrA-000, and the two mutants UvrA-100 (K37A) and UvrA-010 (K353A) were purified from UNC522/pUNC1940, UNC522/pUNC1940-100, and UNC522/pUNC1940-010, respectively, with minor modifications of the method of Thomas et al. (1985). Preliminary characterization of UvrA-001 (K646A) and UvrA-101 (K37A–K646A) overproducers revealed that these mutants have a strong propensity toward inclusion body formation and that soluble protein was undetectable when cultures were grown at 37 °C. Consequently, these mutants were purified by a different procedure. Cells carrying the mutant plasmids were grown at 26 °C to minimize inclusion body formation. Cell-free extract was prepared by freeze–thaw and sonication followed by two successive centrifugations at 20000*g* and 100000*g*. During these centrifugations, ~95% of the mutant proteins sedimented with the cellular debris. The clarified supernatant was applied to a 5-g single-strand DNA-cellulose column equilibrated with 0.1 M KCl/core. The column was washed extensively with column buffer, and the mutant UvrA proteins were eluted with 2 M KCl/core. The peak fractions were combined and dialyzed overnight against 0.1 M KCl/core to selectively precipitate mutant UvrA. The precipitate was collected by centrifugation, resuspended in 0.5 M KCl/core, and dialyzed into storage buffer. Purity of the mutant proteins

prepared in this manner was usually greater than 85%.

Because of the decreased solubility of the K646A mutant, additional mutations at K646 were constructed. The rationale for making the two mutants UvrA-002 (K646R) and UvrA-003 (K646M) was that Arg may be isofunctional and Met isosteric with Lys and, therefore, it was thought that one or both of these substitutions would not perturb the folding and/or tertiary structure of UvrA and consequently not promote inclusion body formation. These proteins, however, were indistinguishable from UvrA-001 both in terms of their in vivo activities and also in terms of their low solubility (data not shown) and, therefore, were not studied further.

Protein concentration was determined by the method of Bradford (1976) using the Bio-Rad kit, and confirmed by densitometric scanning of a Coomassie blue stained SDS–polyacrylamide gel containing each mutant protein and a highly purified UvrA standard.

ATPase Assay. The ATPase activity of UvrA was assayed by the method of Scott et al. (1977) with minor modifications. Reaction mixtures (50 μL) contained 2 μCi of [^{3}H]ATP (1.3 μM), nonradioactive ATP from 10 to 500 μM, and the indicated concentrations of UvrA. Reactions were incubated at room temperature such that no greater than 15% of the substrate was hydrolyzed. ATP hydrolysis was quantified by spotting 2 μL of the reaction mixture on a TLC plate spotted with 20 nmol each of nonradioactive ATP and ADP. The plates were developed and analyzed as described previously (Scott et al., 1977).

Nucleotide Binding. Binding of nucleotides to UvrA was measured by two methods: the equilibrium gel filtration technique of Hummel and Dreyer (1962) and the rate of dialysis technique of Colowick and Womack (1969).

Equilibrium gel filtration was conducted as follows. A 30-mL column of P-10 was equilibrated at room temperature with buffer containing 50 mM Tris-HCl, pH 7.5, 300 mM KCl, 10 mM $MgCl_2$, 1 mM dithiothreitol, 6.5% glycerol, 20 μCi of [^{3}H]ADP (25.4 Ci/mmol), and non-radioactive ADP at the indicated concentrations. UvrA (~3 nmol) was incubated at 23 °C for 10 min in 500 μL of the same buffer and then loaded onto the column. The column was developed with the same buffer at a rate of 10 mL/h. Fractions of 420 μL were collected, 400 μL of which was mixed with 5 mL of Scintiverse I (Fisher), and the radioactivity was determined by scintillation counting. In addition, the protein concentration in each fraction was determined by the Bradford method. The picomoles of nucleotide and protein was measured over the whole peak, and the mole ratio was used to determine the binding stoichiometry. The Hummel–Dreyer method was also used to measure binding to ATP. However, because of the relatively low affinity of UvrA to ATP as compared to ADP, it was not possible to use this technique to determine the ATP binding stoichiometry. Instead, binding with UvrA-000 and UvrA-100 was conducted at 0.1 μM ATP with 20 μCi of [^{3}H]ATP (30 Ci/mmol) as tracer. In addition, to prevent complications that would arise from ATP hydrolysis, we conducted these binding experiments at 4 °C.

The rate of dialysis technique (Colowick & Womack, 1969) utilizes a specially designed chamber consisting of two cylindrical reservoirs separated by a semipermeable membrane. A 550-μL reaction mixture containing 50 mM Tris-HCl, pH 7.5, 300 mM KCl, 10 mM $MgCl_2$, 1 mM dithiothreitol, 100 μg/mL bovine serum albumin plus 3.8 μM UvrA, and 0.2 μM [^{3}H]ADP was incubated for 10 min at 23 °C and then was loaded into the top reservoir of the dialysis chamber. Buffer containing 50 mM Tris-HCl, pH 7.5, 300 mM KCl, 10 mM $MgCl_2$, 1 mM dithiothreitol, and 10% glycerol was passed through the bottom chamber by gravity, and 2-mL fractions were collected. At 15-fraction intervals, the nonradioactive ADP concentration was increased to compete off bound [^{3}H]ADP. Radioactivity in each fraction was determined by scintillation counting. The ADP bound for a given total ADP concentration was calculated by taking the ratio of radioactivity in subsaturating fractions and dividing by the radioactivity in fractions obtained with saturating cold ADP.

Table I: In Vivo Complementation by UvrA Walker A and B Mutants at 150 erg/mm^2 [a]

protein	relative survival	protein	relative survival
000	7.9×10^{-1}	D238N	4.4×10^{-1}
100	4.4×10^{-3}	D513N	6.3×10^{-2}
010	7.8×10^{-1}	D857N	2.6×10^{-1}
001	1.5×10^{-4}	*uvrA*:Tn10	4.0×10^{-7}
101	3.0×10^{-5}		

[a] Serial dilutions of a stationary culture of UNC522 (*uvrA*:Tn10) expressing each of the mutant *uvrA* genes were plated and irradiated with 15 J m^{-2} of 254-nm light. After 18–24 h at 37 °C, the number of colonies was determined and multiplied by the dilution factor to yield the number of survivors.

(A)BC Excinuclease Assays. Binding of UvrA and UvrB was probed by DNase I footprinting using a 137 bp psoralen monoadducted substrate (Van Houten et al., 1987) and by loading of UvrB onto UV-irradiated pBR322 measured by gel exclusion chromatography on a 12-mL AcA22 column (Orren & Sancar, 1989). Nicking of 5′ terminally ^{32}P-labeled UV-irradiated DNA by (A)BC excinuclease was assayed by separating the reaction products on 8% polyacrylamide sequencing gels (Sancar & Rupp, 1983). Substrate for this nicking assay was a 107 bp DNA fragment gel purified from a *Hae*III digest of 1.2 μg of pIBI24N end-labeled with [γ-^{32}P]ATP and T4 polynucleotide kinase. Gel filtration chromatography on AcA-34 resin to detect UvrA–UvrB interactions was carried out as described previously (Orren & Sancar, 1989).

Results

Point Mutations in Conserved Residues of Walker A and B Sequences. Figure 1 shows the segmental organization of UvrA as proposed by Doolittle et al. (1986). According to this scheme, UvrA is made up of three ATPase "A segments" and three "B segments" interspersed with zinc fingers. An A segment and a B segment which contain the Walker A and B sequences, respectively, are proposed to fold into a functional ATPase domain. To test whether UvrA has three ATP binding/hydrolysis domains, as predicted from the sequence, the most conserved residues in Walker's A and B sequences, lysine and aspartic acid, respectively, were replaced with nonconservative residues by site-specific mutagenesis. As shown in Figure 1, Lys was substituted with Ala, and Asp was replaced by Asn. In addition to these substitutions, K646M and K646R constructs were made and partially characterized.

In Vivo Repair Activity of UvrA Point Mutants. The effect of the mutations on UvrA function was investigated by inserting a plasmid carrying the mutant gene into UNC522 (*uvrA*::Tn10) and testing for complementation of the UvrA deficiency by measuring the UV sensitivity of the resulting mutant. The results are summarized in Table I. Surprisingly, substitution of any of the Asp residues with Asn has only a subtle effect on the complementing activity of the mutant proteins. In contrast, changing the invariant lysines to Ala had a striking effect in two out of three mutants; K37A and K646A are noticeably defective in complementing activity while K353A has a wild-type phenotype. The double-mutant UvrA-101 (K37A-K646A) has only minor, but reproducible,

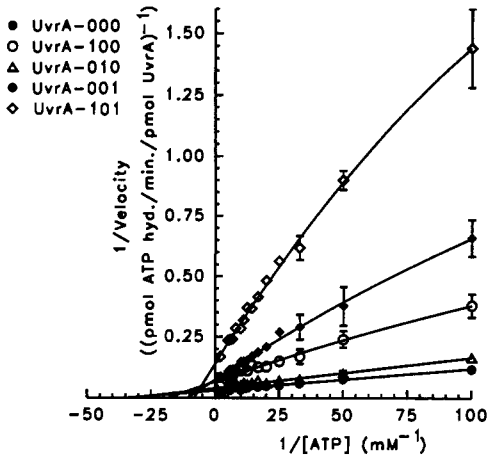

FIGURE 2: Lineweaver–Burk analysis of UvrA's Walker A point mutant ATPase activity. Fifty-microliter reactions in ATPase buffer (see Materials and Methods) contain 67 pmol (2 μCi) of [^{3}H]ATP, 0.7 pmol of UvrA, and from 10 to 500 μM cold ATP. Reactions were started by the addition of UvrA and were incubated at room temperature for the times required to achieve 10–15% maximal ATP hydrolysis (i.e., 30 min–3 h). Reactions were quenched by spotting on TLC plates.

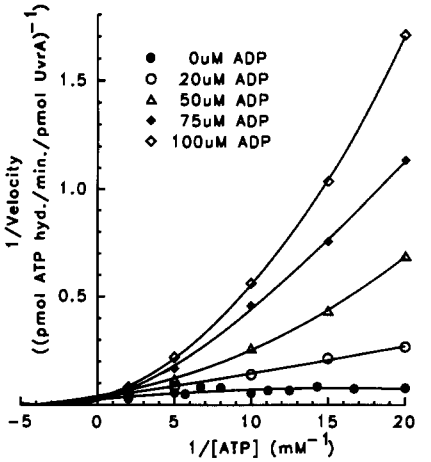

FIGURE 3: ADP inhibition of UvrA's ATPase activity. Each 50-μL reaction was in ATPase buffer including 67 pmol (2 μCi) of [^{3}H]ATP, 2.8 pmol of UvrA, and 10–500 μM ATP. ADP inhibition was measured by including 20, 50, 75, or 100 μM ADP in the reaction mixtures as indicated. Reactions were performed at room temperature for the times required to hydrolyze at most 10–15% of the [^{3}H]ATP (15–120 min) and were quenched by spotting 2 μL on TLC plates. The data are analyzed on a Lineweaver–Burk plot.

Table II: ATPase Activity of Walker A Point Mutants: Summary of Kinetic Constants

protein	V_{max}[a]	K_m (μM)	V_{max}/K_m
000	32.5	29.6	1.10
100	15.0	55.9	0.27
010	28.3	31.3	0.90
001	13.8	92.6	0.15
101	7.4	123.5	0.06

[a] V_{max} = picomoles of ATP hydrolyzed per minute per picomole of UvrA.

Table III: Hill Coefficients for Walker A Point Mutants

protein	$n_{(no\ effector)}$	$n_{(ADP)}$[a]
000	0.94	1.51 ± 0.13
100	0.98	1.06 ± 0.13
010	1.02	1.56 ± 0.16
001	1.01	1.36 ± 0.05
101	1.01	1.10 ± 0.04

[a] $n_{(ADP)}$ is the mean Hill coefficient obtained by averaging the n value derived for each concentration of ADP tested. The error expressed here is one standard deviation.

complementing activity. These data demonstrate the importance of the A1 and A3 segments and may be taken as evidence that UvrA has two ATP active sites, one involving K37 and one involving K646. Also, the lysine residues in two of the Walker A sequences are of vital importance for the in vivo functions of UvrA while the Asp residues in the Walker B sequences are apparently largely replaceable.

Kinetic Studies with Wild-Type and Mutant UvrAs. Since replacement of Asp residues in Walker B sequences did not dramatically affect the phenotype, we concentrated our in vitro work on mutants of the invariant lysines in the Walker A sequences. Wild-type UvrA as well as UvrA-100, UvrA-001, UvrA-010, and UvrA-101 was purified and tested for activity.

For a quantitative comparison of the activities of wild-type and mutant proteins, it is important that protein preparations of near-identical purity be tested. Wild-type UvrA, UvrA-100, and UvrA-010 displayed the same solubility and chromatographic properties and were purified by the same procedure. However, preliminary characterization of UvrA-001 and UvrA-101 overproducers revealed that these mutants have a strong tendency to form inclusion bodies and that only a small fraction of the overproduced protein was soluble when cultures were grown at 37 °C (data not shown); therefore, cells were grown at 26 °C to minimize inclusion body formation. The proteins were isolated by a different procedure from UvrA-000, UvrA-100, and UvrA-010 as described under Materials and Methods. The mutant proteins purified in this manner were comparable to wild type in purity, allowing for a quantitative comparison of their activities.

Figure 2 shows the Lineweaver–Burk plots for the ATPase activity of UvrA and its mutant derivatives, and Table II summarizes the kinetic constants obtained from these plots. The slight nonlinearity suggests negative cooperativity; however, analysis of these data on a Hill plot does not support this (see below). Inspection of the kinetic constants shows that while UvrA-010 is comparable in activity to wild type, both UvrA-100 and UrvA-001 show a decrease in their V_{max} and an increase in their K_m values. As a result, the specificity constant (V_{max}/K_m) for these mutants shows a decrease of 75% and 86% for UvrA-100 and UvrA-001, respectively. Likewise, UvrA-101 shows a drastic increase in K_m and a decrease in V_{max} such that the specificity constant is only 5% of the value of the wild-type protein. These results suggest that both Lys37 and Lys646, but not Lys353, are involved in the ATPase functions of UvrA.

To better define the individual roles of Lys37 and Lys646 in the ATPase activity, we conducted inhibition studies with ADP. Seeberg and Steinum (1982) have previously reported that ADP is a competitive inhibitor of UvrA's ATPase activity. Our results, shown in Figure 3 are consistent with this report but differ in that our data indicate that ADP promotes positive cooperativity. Because of the nonlinearity of the Lineweaver–Burk plots, the values of K_i cannot be extrapolated directly from the slopes in Figure 3. Instead, K_i was determined from the x axis of a graph of $K_{m,app}$ vs [ADP] (Hill replot; Figure 4). Values for $K_{m,app}$ for this graph were obtained from plots of log $(v/V_{max} - v)$ vs log [ATP] for each [ADP] and were taken to be the ATP concentrations where $v/(V_{max} - v) = 1$. As is apparent from Figure 4, the Hill replot is biphasic with the two asymptotes intercepting the x axis at $K_i = 5$ and 50 μM.

Values for Hill coefficients of wild-type and mutant UvrA proteins are presented in Table III. For UvrA-000, the Hill coefficient at [ADP] = 0 μM is $n = 0.94$ whereas the average

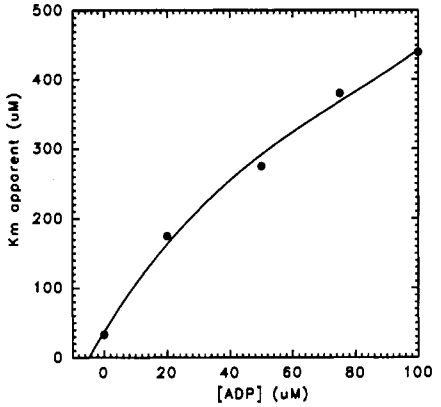

FIGURE 4: Hill replot of UvrA's ATPase activity. Data from Figure 3 are analyzed on Hill plots. The $K_{m,app}$ values were extrapolated as the [ATP] corresponding to $v/(V_{max} - v) = 1.0$ for each [ADP]. The $K_{m,app}$ values for UvrA-000 were plotted vs [ADP] to yield the Hill replot shown here. Asymptotes are constructed for the linear portions of the curve (i.e., at [ADP] = 0 μM and at [ADP] = 100 μM), and the K_i values are extrapolated from the intersection of the x axis by each asymptote.

value for the Hill coefficient is $n = 1.51$ in the presence of ADP, consistent with the observed nonlinearity in the Lineweaver–Burk plots. These data show that while UvrA-000, UvrA-010, and UvrA-001 exhibit positive cooperativity with $n \sim 1.5$, this cooperativity is viturally eliminated by mutagenizing K37; i.e., $n = 1.06$ for UvrA-100 and $n = 1.10$ for UvrA-101. These data indicate that UvrA has two nucleotide binding sites, one involving K37 and one that includes K646, and furthermore that the two sites are not equivalent as mutation of K37 eliminates cooperativity while mutation of K646 does not.

Nucleotide Binding. By conducting nucleotide binding studies, we wished to provide supporting evidence for the conclusions of the kinetic experiments, i.e., that UvrA possesses two ATP binding sites. To avoid the complications that would arise from hydrolysis of ATP, we used ADP for these experiments. ADP and ATPγS inhibit the ATPase activity of UvrA competitively and consequently share the same binding sites with ATP. It is reasonable, therefore, to expect that binding measurements with these nucleotides will accurately reflect the stoichiometry and relative binding affinities of the active sites. Because ADP has ~5-fold higher binding affinity for UvrA than ATPγS (Seeberg & Steinum, 1982), most of our binding measurements were performed with ADP.

Binding experiments were done exclusively with UvrA-000 and UvrA-100; UvrA-010 was not studied because in all aspects it behaves like the wild-type protein. Binding to UvrA-001 and UvrA-101 was not measured because of the unavailability of quantities of these proteins sufficient for binding experiments. Figure 5A shows a typical elution profile for UvrA-000 in a Hummel–Dreyer-type experiment, and Figure 5B represents a hyperbolic saturation curve for UvrA-000 and UvrA-100, which was generated from a series of Hummel–Dreyer profiles such as shown in Figure 5A. The Scatchard plot of the saturation curve (Figure 5C) yields a straight line with a slope and x-axis intercept which yield a K_D of 0.25 μM and a binding stoichiometry [$r_{(sat)}$] of 0.57 ADP/UvrA monomer, respectively. Further, both UvrA-000 and UvrA-100 have indistinguishable ADP binding affinities and stoichiometries.

Because mutation of Lys37 has no effect on UvrA's ADP binding affinity or stoichiometry, it is unclear whether ADP is binding to the carboxy-terminal domain (i.e., A3) or, alternatively, whether ADP binds to the amino-terminal domain (i.e., A1) and Lys37 has no role in this activity. To differentiate these possibilities, we measured binding to ATP at 0.1 μM (at 4 °C to minimize ATP hydrolysis). Figure 5D shows that UvrA-100 is clearly defective in binding ATP as compared to UvrA-000. Because the ADP binding stoichiometry is 1/dimer (see below) and because ADP inhibits UvrA's ATPase activity competitively, we conclude that under conditions of binding only, ADP and/or ATP bind exclusively to the amino-terminal domain. Further, the role of Lys37 is to provide the γ-phosphate contact with ATP.

Because kinetic data indicated two binding sites per UvrA functional unit, we reasoned that a low-affinity binding site could have been missed because of limitations in the sensitivity of the Hummel–Dreyer analysis. Therefore, we also measured binding with the rate of dialysis technique of Colowick and Womack (1969) which can detect binding to low-affinity sites. A representative run for UvrA-000 is shown in Figure 6A and a Scatchard plot of the data in Figure 6B. Again, the binding is hyperbolic with no evidence for multiple nucleotide binding sites; that is, increasing amounts of low concentrations of competing ADP incrementally approach saturation without reaching a plateau at an intermediate off rate. The Scatchard plot is linear and yields $K_D = 0.7$ μM and $r_{(sat)} = 0.45$, in reasonable agreement with the values obtained by the Hummel–Dreyer method.

It is important to emphasize that high concentrations of ADP (i.e., [ADP] > 20 μM) do not alter the value for the binding stoichiometry; that is, binding never exceeds 0.5 ADP/UvrA monomer even at [ADP] as high as 50 μM.

Thus, considering all available data, we conclude that in the absence of ATP hydrolysis ADP saturates UvrA at a stoichiometry of 0.5/monomer. Since the native protein is a dimer (Orren & Sancar, 1988, 1989; Oh et al., 1989) with an association constant of $K_A \sim 10^8$ M^{-1} (Orren & Sancar, 1988) under the conditions of our binding studies (6 μM UvrA), essentially all of the protein is in the dimer form, and, therefore, it is more accurate to consider the binding stoichiometry as 1 mol of ADP/mol of UvrA dimer. Indeed, when the specific activity of UvrA is measured as a function of protein concentration (Figure 7), there is a striking dependence of ATPase activity on concentration over the range 1–100 nM with an inflection point at around 10 nM. These data are consistent with the reported monomer–dimer equilibrium association constant (Orren & Sancar, 1988) and, furthermore, suggest that the ATPase activity is either strictly dependent upon or greatly stimulated by its dimerization. Significantly, a theoretical ATPase activity versus [UvrA] curve based on a dimerization constant of 10^8 M^{-1} and assuming that the UvrA monomer lacks ATPase activity is in excellent agreement with the experimental data. We, therefore, favor the view that dimerization is essential for the protein's ATPase activity.

DNA Incision and Binding. When the mutant UvrA proteins were used to reconstitute (A)BC excinuclease, we found that the nuclease reconstituted with UvrA-010 had activity identical with that reconstituted with the wild-type protein. In contrast, UvrA-100 had greatly diminished and UvrA-001 and UvrA-101 had barely detectable in vitro complementation activities (Figure 8). According to the model of Orren and Sancar (1989, 1990), UvrA makes a $(UvrA)_2(UvrB)_1$ complex, and this complex delivers UvrB to the damage site guided by UvrA's affinity for damaged DNA. Therefore, diminished overall nuclease activity could be due to either decreased affinity of UvrA for damaged DNA or the inability of UvrA to deliver UvrB to the damage site. To distinguish between

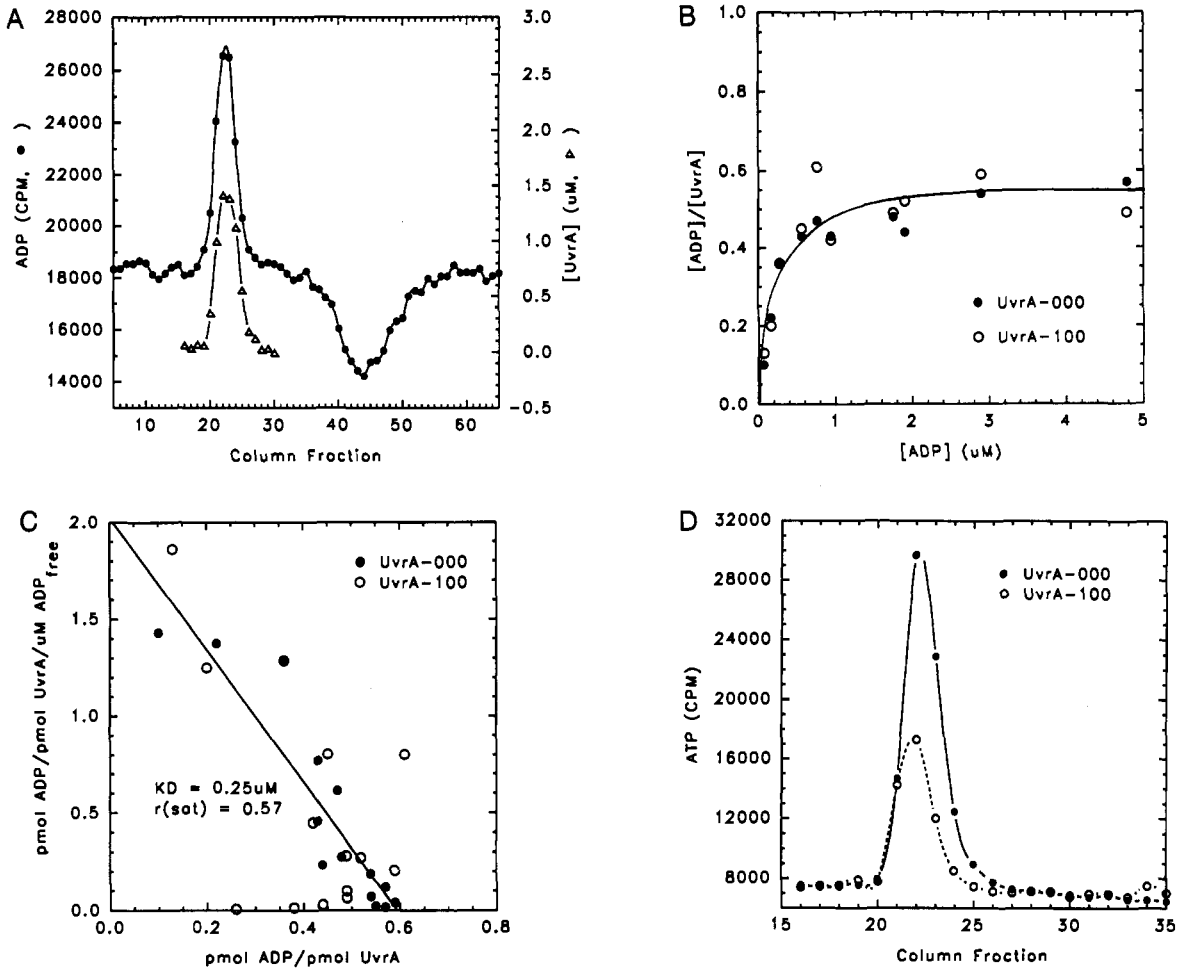

FIGURE 5: Nucleotide binding of UvrA by equilibrium gel filtration. (A) A representative column profile. The column was equilibrated with buffer containing 1.75 μM ADP (see Materials and Methods for column specifications). 3.2 nmol (330 μg) of UvrA was equilibrated with the column buffer at room temperature for 15 min in a 500-μL volume prior to being loaded onto the column. The total micromolar ADP bound in each fraction was determined by subtracting the background cpm (which corresponds to 1.75 μM ADP) from the cpm in each fraction comprising the protein peak and summing each net cpm value. The protein concentration in each fraction comprising the peak was determined by the Bradford assay using a commercial preparation of BSA as a standard. Each column run such as this constitutes one point on the saturation curve B. (B) ADP binding saturation curve. Data shown in (A) are plotted as the [ADP]/[UvrA] for each ADP concentration. Points were determined from 0.07 to 50 μM; the points to 5 μM [ADP] are shown here. UvrA-000 points were obtained with 3.2 nmol of protein while UvrA-100 points are from measurements with 3.0 nmol of protein. (C) Scatchard plot of equilibrium gel filtration binding data. The data from (B) plotted as the binding stoichiometry (r) divided by the free nucleotide concentration vs r. The free nucleotide concentration in a fraction is taken as the starting ADP concentration for a given column run. The data shown here include all the points in (B) and include those obtained at higher ADP concentrations (up to 35.8 μM). Higher concentrations of ADP do not result in a nucleotide peak which can be quantitated accurately against the background. (D) Equilibrium gel filtration profile for ATP binding. Binding and column conditions were essentially as described in (A) except that here binding was measured to 0.1 μM ATP.

these two possibilities, we conducted DNase I footprinting experiments (Figure 9). In contrast to an earlier report (Van Houten et al., 1988), ATP does not appear to increase the affinity of UvrA for the DNA substrate; rather, it results in the "tightening" of the footprint by reducing nonspecific binding (Figure 9A). UvrA-100 and UvrA-001 differ from wild-type UvrA in that both are deficient in this ATP-dependent "tightening" of the footprints (more obvious in UvrA-001 in the figure but reproducibly seen with both mutants in several repeats). The specific binding affinity of UvrA-100 is indistinguishable from wild type, and that of UvrA-001 is lower by about a factor of 2. (In comparing the footprints, allowance should be made for the unequal digestion by DNase I and/or different level of exposure of the autoradiograms.) Damage specificity for these mutants was confirmed by gel retardation experiments using a randomly damaged 107 bp DNA fragment (data not shown). Thus, while there are some differences in the affinity of wild-type and UvrA-001 proteins for substrate DNA, the differences are not sufficient to account for the drastic decrease in incision activity of the excinuclease, and, therefore, the latter must be due to a more pronounced effect on the delivery of UvrB to the damage site.

Loading of UvrB onto Damaged DNA. The loading of UvrB onto DNA by wild-type and mutant UvrAs was tested by two methods: DNase I footprinting and gel exclusion chromatography. DNase I footprints of UvrA obtained in the presence of ATP and UvrB reveal a hypersensitive site at the 11th phosphodiester bond 5′ to the adduct (Van Houten et al., 1987). Since this site does not form in the absence of UvrB, it has been suggested that it signals the presence of UvrB at the adduct site. This is clearly seen in Figure 9A with wild-type UvrA and to a much lesser degree in Figure 9B with UvrA-100; there is no hypersensitive site (UvrB footprint) detectable with UvrA-001 (Figure 9C). In fact, a comparison of the level of incision observed in Figure 8 and the intensity of the hypersensitive band and UvrA footprint in Figure 9 shows a close correlation between the intensity of incision and that of the hypersensitive band, but no such correlation exists between the specific affinity of UvrA and incision, suggesting

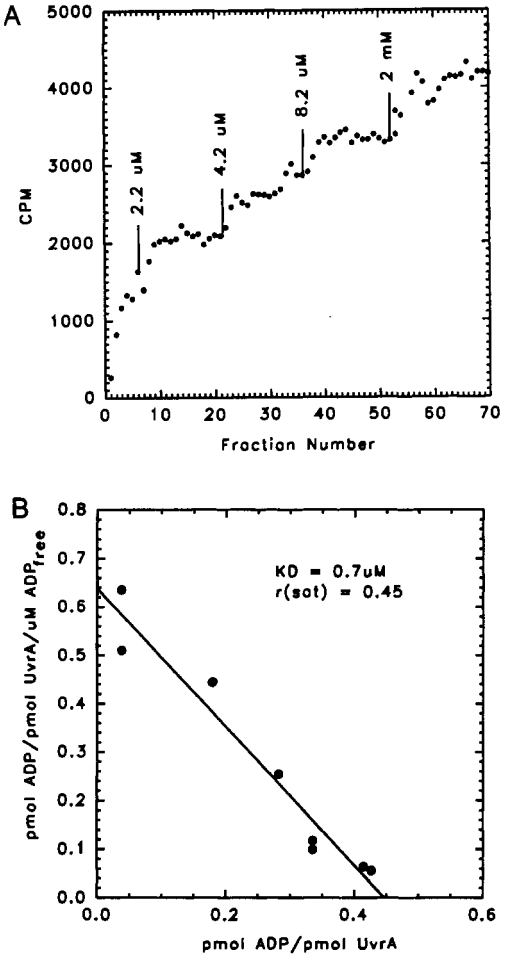

FIGURE 6: ADP binding by the rate of dialysis. (A) ADP binding profile from a single run. 300 μg of UvrA was dialyzed against buffer containing 50 mM Tris, pH 7.5, 300 mM KCl, 10 mM $MgCl_2$, 1 mM DTT, 100 μg/mL BSA, and 10% glycerol. After equilibration of UvrA with the buffer, [^{3}H]ADP was added to 0.2 μM. The protein–ADP reaction mixture was loaded into the top chamber as described under Materials and Methods, and buffer was passed through the bottom chamber. Cold ADP was added to the top chamber at the concentrations and fractions indicated. (B) Data from two separate rate of dialysis runs as shown in (A) are plotted as described by Scatchard (1949).

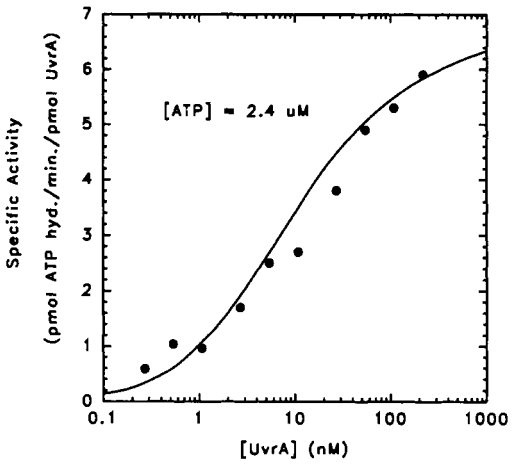

FIGURE 7: ATPase activity as a function of UvrA concentration. Fifty-microliter reactions were performed at room temperature in ATPase buffer (see Materials and Methods for its composition) containing 1.25 μM ATP, 2 μCi of [^{3}H]ATP (1.18 μM), and UvrA from 270 pM to 216 nm, as indicated, and for times such that the picomoles of ATP hydrolyzed per UvrA per minute is held constant (i.e., from 200 min to 15 s). Protein was prewarmed in reaction buffer for 15 min at room temperature, and reactions were started by adding the ATP (^{3}H and cold together). Reactions were quenched by spotting 2 μL on a TLC plate. The symbols are actual data points while the curve is theoretical and is based on the assumption that dimers form with a K_D = 10 nM and have full ATPase activity while monomers have no ATPase activity.

that the defective step with (A)BC excinuclease with mutant UvrA is the delivery of UvrB to the damage site. This conclusion is supported by direct measurements of UvrB loading by wild-type and mutant UvrAs using gel exclusion chromatography. The results are shown in Figure 10. In the presence of catalytic amounts of UvrA, nearly stoichiometric [see Orren and Sancar (1989)] levels of UvrB are loaded onto UV-damaged pBR322 by wild-type protein and UvrA-010. The loading is drastically decreased with UvrA-100 and barely above background level with UvrA-001 and UvrA-101. Thus, we conclude that mutations at either K37 or K646 affect the ATPase activity of UvrA and that this decreased activity drastically reduces its ability to deliver UvrB to the damage site. There are two possibilities for the role of ATP hydrolysis in the UvrA-mediated loading of UvrB: (1) ATP hydrolysis is essential for formation of A_2B_1 complexes (Orren & Sancar, 1989) or (2) ATP hydrolysis is required for the transfer of UvrB from A_2B_1 complexes onto damaged DNA. To test the former possibility, we assayed the association of UvrA with UvrB by gel filtration chromatography. We found that association of the mutant UvrAs, 100 and 001, with UvrB was drastically reduced as compared to the wild-type protein (data not shown).

Discussion

By comparing the sequences of a number of ATPases known to have Walker A and B sequence motifs, Doolittle et al. (1986) and Higgins et al. (1986) discovered that the sequence homology extended well beyond the A and B motifs to cover 100–150 amino acids each around the A and B sequences. These were termed the A and B segments, and it was proposed that a prototype ATPase would be made of one A and one B segment fused together to fold into an ATPase domain. Each ATPase was presumed to contain additional components to link the ATP hydrolysis to a particular function (e.g., transport). Although the original lists contained, in addition to UvrA, only a few membrane transport proteins, very interesting proteins such as Mdr (multidrug resistance; Gros et al., 1986) and CFTR (cystic fibrosis transmembrane regulator; Foote et al., 1989) have been added to the list. More recently, a more restrictive UvrA superfamily has been proposed (Gorbalenya & Koonin, 1990).

UvrA contains three A (A1–A3) and three B (B1–B3) segments set apart by three zinc finger motifs. The second of these zinc finger sequences contains only two of the four cysteines required for zinc chelation and, therefore, is presumed to be nonfunctional. The B1 and A2 sequences are severely truncated, and, therefore, it has been proposed that A1–B2 and A3–B3 are folded into two functional domains, each incorporating its own zinc finger.

We have conducted site-specific mutagenesis on the two invariant residues of the Walker A and B sequences, Lys and Asp, respectively, to test the predictions from the amino acid sequence. It has been proposed on the basis of structural (Pai et al., 1977; Fry et al., 1985, 1988) and affinity labeling studies that the conserved Lys in the Walker A sequence interacts with either the α- or the γ-phosphate of ATP. Similarly, it has been proposed that the Asp in the Walker B sequence coordinates Mg^{2+}, thus facilitating the positional change in coordination of Mg^{2+} as the reaction proceeds from Mg-ATP to Mg-ADP (Fry et al., 1986). Site-specific mutagenesis studies, in general, have confirmed the importance of these residues for ATPase

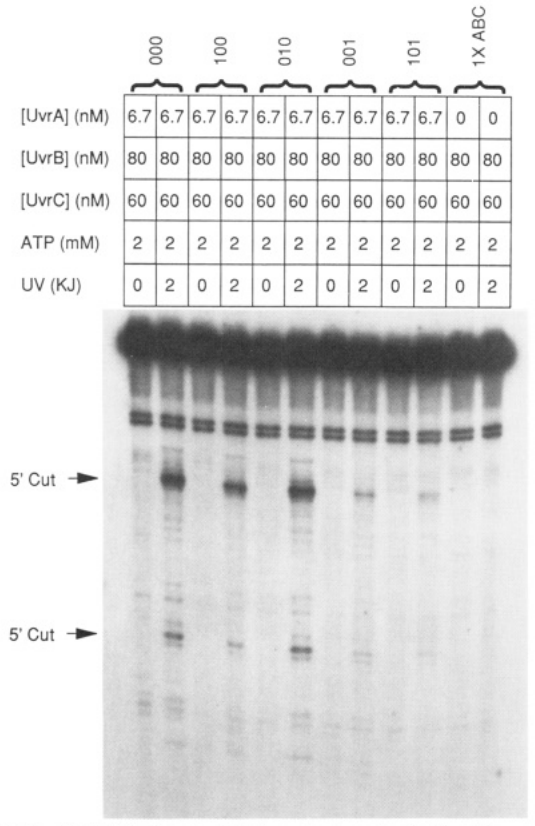

FIGURE 8: UvrA Walker A point mutant mediated incision of UV-irradiated 107 bp DNA fragment. Twenty-microliter incision reactions contained ~1500 cpm of the DNA fragment (UV or non-UV as indicated), 6.7 nM UvrA, 80 nM UvrB, 60 nM UvrC, and 2 mM ATP in (A)BC excinuclease buffer supplemented with 10% glycerol. Reactions were incubated at room temperature for 30 min, quenched by precipitating the DNA with EtOH at −80 °C. DNA was suspended in formamide plus dyes and electrophoresed on an 8% sequencing polyacrylamide gel. Bands were visualized by autoradiography. KJ, kilojoules per square meter. Since the fragment is 5′ labeled, of the two fragments resulting from incisions on the 5′ and 3′ sides of UV photoproducts, only the one resulting from the 5′ incision woud be detectable by autoradiography. The doublet near the top of the gel in all of the lanes is due to a minor contaminant of the 107 bp substrate.

function. Substitution of Lys by another amino acid in *E. coli* F_1 ATPase (Parsonage et al., 1987) and yeast RAD3 protein (Sung et al., 1988) resulted in complete loss of complementing activity in vivo and of ATPase activity in vitro. Substitution of Asp of the Walker B sequence in the β subunit of F_1 ATPase of *E. coli* (Al-Shawi et al., 1988) and of a thermophilic ATPase (Yohda et al., 1988) also resulted in >90% loss of activity. It was, therefore, surprising that our K37A and K646A mutants had significant complementing activities in vivo and that D513N and D857N mutations had little effect on activity. It is likely that mutation of either Lys37 or Lys646 does not totally eliminate the respective activities. Alternatively, it is possible that complete elimination of one activity still yields a protein of partial activity.

Our site-specific mutagenesis data are entirely consistent with the native form of UvrA possessing two ATPase sites; that is, kinetic data with ADP as a competitive inhibitor yield $n = 1.5$ for the Hill coefficient. This positive cooperativity between active sites is eliminated by mutagenesis of K37 (i.e., for UvrA-100, $n = 1.06$, and for UvrA-101, $n = 1.10$). However, in the K646A mutant, $n = 1.36$, indicating that only the ATPase activity associated with the A1 sequence is responsible for the positive cooperativity.

In contrast to site-specific mutagenesis, nucleotide binding measurements by equilibrium methods yielded 0.5 binding site per UvrA monomer. This, combined with hydrodynamic measurements indicating that the native state of UvrA is a dimer with an association constant $K_A \sim 10^8\ M^{-1}$, suggests that the active form of UvrA is a dimer possessing one nucleotide binding site. Indeed, dilution of UvrA so as to shift the monomer–dimer equilibrium in the direction of the monomer resulted in a drastic decrease in the protein's specific activity, indicating that dimerization is essential for the protein's ATPase function. We do not consider the kinetics and binding data to be contradictory, however, as binding is a measure of the ratio of nucleotide to protein while kinetics measure the types (with regard to affinity and efficiency) of active sites in the active form of an enzyme, in this case a UvrA dimer. Therefore, a model consistent with both kinetic and binding data would be that a UvrA dimer binds one ATP molecule at a site which involves K37 and that hydrolysis of a nucleotide at this site activates the second lower affinity ATPase site in the dimer which involves K646. Alternatively, as reported by Orren and Sancar (1988), ADP stabilizes UvrA dimerization; therefore, it is possible that an ADP-dependent shift in the monomer–dimer equilibrium may be responsible for this positive cooperativity. Replacement of K37 by site-specific mutagenesis eliminates the positive cooperativity, indicating that this site has an allosteric function. However, the mutant protein still binds ADP with the same affinity as the wild-type protein, indicating that K37 is not essential for binding to this nucleotide. In contrast, ATP binding is significantly reduced in this mutant, and, therefore, we conclude that this amino acid is responsible for γ-phosphate contact with ATP. The site involving K646 is important for catalysis but apparently has no allosteric effect.

That UvrA dimers have maximal ATPase activity and that UvrA binds nucleotide with a stoichiometry of 1 per dimer imply that nucleotide binding sites form at the interface of the monomers or alternatively at a single site on a UvrA monomer (i.e., half-of-the-sites reactivity). The absence of negative cooperativity, by Hill analysis of ATPase data as well as the hyperbolic ADP binding curve, suggests that the active site forms across the interface of the two monomers. Further, these data also strongly suggest that dimerization occurs in a head-to-head, tail-to-tail arrangement to create two non-equivalent active sites. This has been verified by the demonstration that the purified amino-terminal domain (monomer $M_r = 70000$) has a native molecular weight of 126000 by gel filtration chromatography and that the amino- and carboxy-terminal domains do not interact noncovalently (Myles & Sancar, 1990).

Our data also shed some light on the role of the ATPase function of UvrA in the overall reaction catalyzed by (A)BC excinuclease. Previous work has shown that UvrA has two functions; recognition of DNA damage and delivery of the UvrB subunit to that site. Our results show that neither ATP binding nor hydrolysis is essential for binding to the damage site but that ATP binding/hydrolysis is necessary for delivering UvrB to that site. In this regard, the two ATPase sites (as defined by K37 and K646 mutations) behaved differently. UvrA-100 (K37A) had about 10% of the UvrB loading activity as evidenced by the intensity of the UvrB hypersensitive site with DNase I footprinting and direct measurement by gel exclusion while UvrA-001 (K646A) had about 1% of this activity. Further, (A)BC excinuclease reconstituted with these mutants had incision activities comparable to the loading. Recently, Seeley and Grossman (1989) presented evidence which indicated that the cryptic ATPase of UvrB, which becomes overt in the UvrA–UvrB–DNA complex, was essential

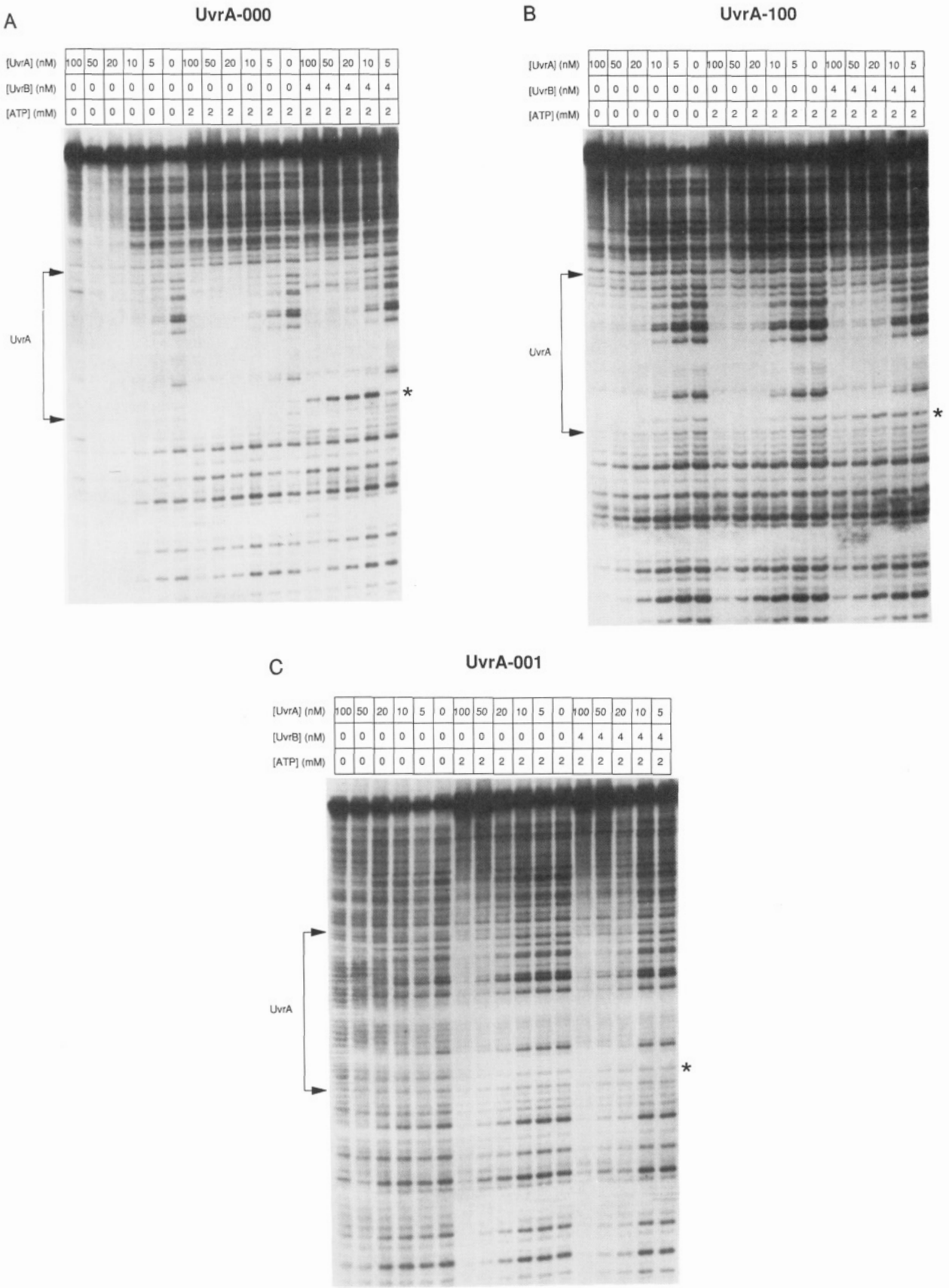

FIGURE 9: DNase I footprinting of UvrA Walker A point mutants. Footprinting reactions are 50 μL and were performed in (A)BC excinuclease buffer containing ~2000 cpm of DNA and the concentrations of UvrA indicated. Where indicated, 4 nm UvrB and/or 2 mM ATP were also included. Reactions were incubated at room temperature for 25 min prior to the addition of 2.5 μL of DNase I (150 pg/mL in 0.1 M $CaCl_2$); the nuclease digestion was incubated at room temperature for 5 min and quenched by precipitating the DNA with EtOH using 2 μg of calf thymus DNA as carrier. The precipitated DNA was resuspended in 25 μL of 95% formamide dyes (Bromphenol blue, 0.1% w/v, and Xylene cyanol 0.1% w/v) and heated at 90 °C for 5 min. Five microliters was electrophoresed on an 8% sequencing polyacrylamide gel; bands are visualized by autoradiography. (A) UvrA-000; (B) UvrA-100; (C) UvrA-001. The asterisks indicate the position of the DNase I hypersensitive site in the UvrA–UvrB–DNA or UvrB–DNA complexes.

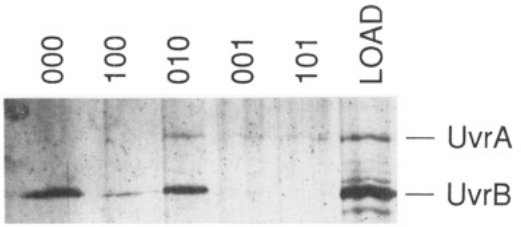

FIGURE 10: Loading of UvrB by UvrA Walker A point mutants. Reactions were performed as described under Materials and Methods. Four hundred microliters of the plasmid-containing fraction from a series of five column runs were heated at 95 °C for 30 min and electrophoresed on a 10% SDS–polyacrylamide gel stained with silver (Bio-Rad kit). Twenty microliters of each load was mixed with 400 μL of column buffer, heated as described for the plasmid fractions, and electrophoresed on the same gel. These samples serve as a control for equivalent protein loading and recovery and also demonstrate that the apparent absence of UvrA in the plasmid fractions is not the result of an electrophoresis artifact.

for loading UvrB onto the damage site although mutation of this ATPase activity apparently has no effect on the UvrA–UvrB interaction. Our results show that UvrA's ATPase activity is essential for this step. However, the two conclusions are not contradictory. The loading of UvrB onto the damaged site involves association of a UvrA dimer with UvrB followed by the loading reaction itself. Both association of the two subunits (Orren & Sancar, 1989) and the loading of UvrB (Van Houten et al., 1988) are ATP dependent. We have found (data not shown) that in UvrA-100 and UvrA-001 the association of UvrA with UvrB is greatly reduced. Thus, it appears that the ATPase activities of both UvrA and UvrB are essential for loading but the two ATPases function at different steps of the overall reaction.

In conclusion, we believe UvrA to have two domains defined by the A1–B2 and A3–B3 segments defined by Doolittle et al. (1986). Each domain has its own zinc finger, and each domain is presumed to fold independently and to have an ATP binding/hydrolysis activity as well as a DNA binding activity conferred by the zinc fingers. This premise is directly addressed in the following paper (Myles & Sancar, 1991).

References

Al-Shawi, M. K., Parsonage, D., & Senior, A. E. (1988) *J. Biol. Chem. 263*, 19633–19639.

Bradford, M. M. (1976) *Anal. Biochem. 72*, 248–254.

Chothia, C. (1975) *Nature (London) 254*, 304–308.

Colowick, S. P., & Womack, F. C. (1969) *J. Biol. Chem. 244*, 774–777.

Dombroski, A. J., Brennan, C. A., Spear, P., & Platt, T. (1988a) *J. Biol. Chem. 263*, 18802–18809.

Dombroski, A. J., LaDine, J. R., Cross, R. L., & Platt, T. (1988b) *J. Biol. Chem. 263*, 18810–18815.

Doolittle, R. R., Johnson, M. S., Husain, I., Van Houten, B., Thomas, D. C., & Sancar, A. (1986) *Nature (London) 323*, 451–453.

Duncan, T. M., Parsonage, D., & Senior, A. E. (1986) *FEBS Lett. 208*, 1–6.

Foote, S. J., Thompson, J. K., Cowman, A. F., & Kemp, D. J. (1989) *Cell 57*, 921–930.

Fry, D. C., Kuby, S. A., & Mildvan, A. S. (1985) *Biochemistry 24*, 4680–4694.

Fry, D. C., Kuby, S. A., & Mildvan, A. S. (1986) *Proc. Natl. Acad. Sci. U.S.A. 83*, 907–911.

Fry, D. C., Byler, D. M., Susi, H., Brown, E. M., Kuby, S. A., & Mildvan, A. S. (1988) *Biochemistry 27*, 3588–3598.

Gorbalenya, A. E., & Koonin, E. V. (1990) *J. Mol. Biol. 213*, 583–591.

Gros, P., Raymond, M., Bell, J., & Housman, D. (1988) *Mol. Cell. Biol. 8*, 2770–2778.

Grossman, L., & Yeung, A. T. (1990) *Photochem. Photobiol. 51*, 749–755.

Higgins, C. F., Hiles, I. D., Salmond, G. P. C., Gill, D. R., Downie, J. A., Evans, I. J., Holland, I. B., Gray, L., Buckel, S. D., Bell, A. W., & Hermodson, M. A. (1986) *Nature (London) 323*, 448–450.

Hummel, J. P., & Dreyer, W. J. (1962) *Biochim. Biophys. Acta 63*, 530–532.

Husain, I., Van Houten, B., Thomas, D. C., & Sancar, A. (1986) *J. Biol. Chem. 261*, 4895–4901.

Kunkel, T. A., Roberts, J. D., & Zakour, R. A. (1987) *Methods Enzymol. 154*, 367–382.

Laemmli, U. K. (1970) *Nature (London) 227*, 680–685.

Lineweaver, H., & Burk, D. (1934) *J. Am. Chem. Soc. 56*, 658–666.

Myles, G. M., & Sancar, A. (1991) *Biochemistry* (second of three papers in this issue).

Navaratnam, S., Myles, G. M., Strange, R. W., & Sancar, A. (1989) *J. Biol. Chem. 264*, 16067–16701.

Oh, E. Y., Claassen, L., Thiagalingam, S., Mazure, S., & Grossman, L. (1989) *Nucleic Acids Res. 17*, 4145–4159.

Orren, D. K., & Sancar, A. (1988) *UCLA Symp. Mol. Cell. Biol. 83*, 87–94.

Orren, D. K., & Sancar, A. (1989) *Proc. Natl. Acad. Sci. U.S.A. 86*, 5237–5241.

Orren, D. K., & Sancar, A. (1990) *J. Biol. Chem. 265*, 15796–15803.

Pai, E. F., Sachsenheimer, W., Schirmer, R. H., & Schulz, G. E. (1977) *J. Mol. Biol. 114*, 37–45.

Parsonage, D., Wile-Mounts, S., & Senior, A. E. (1987) *J. Biol. Chem. 263*, 8022–8026.

Parsonage, D., Al-Shawi, M. K., & Senior, A. E. (1988) *J. Biol. Chem. 262*, 4740–4744.

Rao, R., Pagan, J., & Senior, A. E. (1988) *J. Biol. Chem. 263*, 15957–15963.

Sancar, A., & Rupp, W. D. (1983) *Cell 33*, 249–260.

Sancar, A., & Sancar, G. B. (1988) *Annu. Rev. Biochem. 57*, 29–67.

Sanger, F., Nicklen, S., & Coulson, A. R. (1977) *Proc. Natl. Acad. Sci. U.S.A. 74*, 5463–5467.

Scatchard, G. (1949) *Ann. N.Y. Acad. Sci. 51*, 660–672.

Scott, J. F., Eisenberg, S., Bertsch, L. L., & Kornberg, A. (1977) *Proc. Natl. Acad. Sci. U.S.A. 74*, 193–197.

Seeberg, E., & Steinum, A. L. (1982) *Proc. Natl. Acad. Sci. U.S.A. 79*, 988–992.

Seeley, T. W., & Grossman, L. (1989) *Proc. Natl. Acad. Sci. U.S.A. 86*, 6577–6581.

Seeley, T. W., & Grossman, L. (1990) *J. Biol. Chem. 265*, 7158–7165.

Sung, P., Higgins, D., Prakash, L., & Prakash, S. (1988) *EMBO J. 7*, 3263–3269.

Tabor, S., & Richardson, D. D. (1987) *Proc. Natl. Acad. Sci. U.S.A. 84*, 4767–4771.

Thomas, D. C., Levy, M., & Sancar, A. (1985) *J. Biol. Chem. 260*, 9875–9883.

Van Houten, B., (1990) *Microbiol. Rev. 54*, 18–51.

Van Houten, B., Gamper, H., Sancar, A., & Hearst, J. E. (1987) *J. Biol. Chem. 262*, 13180–13187.

Van Houten, B., Gamper, H., Hearst, J. E., & Sancar, A. (1988) *J. Biol. Chem. 263*, 16553–16560.
Walker, J. E., Saraste, M., Runswick, M. J., & Gay, N. J. (1982) *EMBO J. 1*, 945–951.
Yohda, M., Ohta, S., Hisabori, T., & Kagawa, Y. (1988) *Biochim. Biophys. Acta 933*, 156–164.
Zoller, M. J., & Smith, M. (1983) *Method Enzymol. 100*, 468–500.

Isolation and Characterization of Functional Domains of UvrA†

Gary M. Myles‡ and Aziz Sancar*

Department of Biochemistry and Biophysics, University of North Carolina School of Medicine, Chapel Hill, North Carolina 27599

Received November 8, 1990; Revised Manuscript Received January 15, 1991

ABSTRACT: The sequence of *Escherichia coli* UvrA protein suggests that it may fold into two functional domains each possessing DNA binding and ATPase activities. We have taken two approaches to physically isolate polypeptides corresponding to the two putative domains. First, a 180 base pair DNA segment encoding multiple collagenase recognition sequences was inserted into UvrA's putative interdomain hinge region. This UvrA derivative was purified and digested with collagenase, and the resulting 70-kDa N-terminal and 35-kDa C-terminal fragments were purified. Both fragments possessed nonspecific DNA binding activity, but only the N-terminal domain retained its nucleotide binding capacity as evidenced by measurements of ATP hydrolysis and by ATP photo-cross-linking. Together, the two fragments failed to substitute for UvrA in reconstituting (A)BC excinuclease and, therefore, were presumed to be unable to load UvrB onto damaged DNA. Second, the DNA segments encoding the two domains were fused to the β-galactosidase gene. The UvrA N-terminal domain–β-galactosidase fusion protein was overproduced and purified. This fusion protein had ATPase activity, thus confirming that the amino-terminal domain does possess an intrinsic ATPase activity independent of any interaction with the carboxy terminus. Our results show that UvrA has two functional domains and that the specificity for binding to damaged DNA is provided by the proper three-dimensional orientation of one zinc finger motif relative to the other and is not an intrinsic property of an individual zinc finger domain.

UvrA, which is one of the three subunits of *Escherichia coli* (A)BC excinuclease (Sancar & Sancar, 1988; Selby & Sancar, 1990), is an ATPase and a DNA binding protein with higher affinity for damaged than for undamaged DNA (Seeberg & Steinum, 1982). Analysis of the amino acid sequence of UvrA (Husain et al., 1986) has revealed 3 ATPase A and B segments interspersed with 3 zinc finger motifs each of 21–23 amino acids (Doolittle et al., 1986). It appears that the second zinc finger motif is degenerate and, therefore, has lost its zinc chelating capacity; thus, UvrA contains only 2 mol of Zn^{2+} per monomer apparently chelated by the first and third motifs (Navaratnam et al., 1989). Similarly, of the three pairs of ATPase A and B segments, B1 and A2 appear to be severely truncated (Doolittle et al., 1986). Indeed, mutagenesis of the "invariant" Lys residue in the A2 segment and the invariant Asp residue in the B1 segment had no effect on the protein's in vivo activity. This has led to the proposal that the two ATPase activities of UvrA were made up of A1–B2 and A3–B3 segments, respectively (Myles et al., 1991), and that each of these ATPase units was associated with a zinc finger, A1–B2 with Zn1 and A3–B3 with Zn3, to constitute two domains each with its own DNA binding and ATPase activities.

In this paper, we describe the use of genetic engineering methods to isolate fragments of UvrA containing A1–Zn1–B2 (70 kDa) and A3–Zn3–B3 (35 kDa) sequences. Our results show that each of these fragments constitutes a domain with nonspecific DNA binding activity but that only the A1–Zn1–B2 domain possesses ATPase activity when not physically linked to the carboxy-terminal A3–Zn3–B3 domain.

Materials and Methods

Materials. The wild-type UvrA, UvrB, and UvrC proteins were purified as described previously (Thomas et al., 1985). Collagenase from *Achromobacter iophagus* was purchased from Boehringer Mannheim Biochemicals; it was suspended at 0.12 mg/mL in TEN 7.4 and stored at 4 °C. *Nco*I was obtained from Promega; T4 kinase, bacterial alkaline phosphatase, *Bam*HI, and *Sau*3A were from Bethesda Research Laboratories; and T4 ligase and T4 DNA polymerase were from Bio-Rad.

[2,8-^{3}H]ATP (30 Ci/mmol), [α-^{32}P]ATP (3000 Ci/mmol), and [γ-^{32}P]ATP (7000 Ci/mmol) were from ICN Biomedicals, Inc.; [^{3}H]thymidine (82.4 Ci/mmol) was from New England Nuclear.

Single-strand DNA–cellulose and heparin–agarose affinity resins were from Sigma, AcA-34 gel filtration resin was from IBM Biotechnics, and DEAE-Bio-Gel was from Bio-Rad.

Silver-staining reagents were purchased from Bio-Rad, IPTG and ONPG were from Boehringer Mannheim Biochemicals, and the TLC plates (Polygram cel300 PEI) were from Brinkmann Instruments.

† This work was supported by Grants GM32833 from the National Institutes of Health and PCM8351212 from the National Science Foundation and in part by Grant CTR1872 from The Council for Tobacco Research Inc.

* Correspondence should be addressed to this author.
‡ Present address: Fred Hutchinson Cancer Research Center, 1124 Columbia St., Seattle, WA 98104.

0006-2960/91/0430-3834$02.50/0